well as the strain associated with cage distortions are important factors in the reduction of C_{60}. The simple explanation offered earlier[3] for the structure of $C_{60}H_{36}$ was based on the consideration that 36 is the number of hydrogens required to leave a single unconjugated double bond in each pentagon of C_{60}. We feel that it is not unreasonable to postulate a structure of $C_{60}H_{36}$ as one with four tetrahedrally disposed benzene rings. It is possible that a structure with isolated double bonds first formed transforms to the thermodynamically more stable structure with the benzenoid rings via sigmatropic shifts. Thus with the four symmetrically spaced benzene units in the spheroid, the shape of the cage permits an effective elimination of angle strain at both the sp^2 and sp^3carbon atoms. The overall angular distortions are marginally higher for the T isomer than the T_h form. It appears that the aromatic character of the benzenoid units is responsible for the greater stabilization of the former isomer. It is also likely that under conditions of Birch reduction with *tert*-butanol as the proton source only partial reduction of C_{60} occurs leaving four hexa-substituted benzene rings.

1 Special issue on Buckminster-fullerene, *Acc Chem Res*, 1992, 25, 99

2 Special issue on Fullerenesm, *Indian J Chem*, 1992, **31 A & B**, F1

3 Haufler, R E *et al J Phys Chem*, 1990, **94**, 8634

4 Henderson, H G and Cahill, P A, *Science*, 1993, **259**, 1885.

5 Saunders, M, *Science*, 191, **253**, 330

6 Dunlap, B I, Brenner, D W, Mintmire, J W, Mowrey, R C and White, C T, *J Phys Chem*, 1991, **95**, 5763

7 Guo T and Scuseria, G E, *Chem Phys Lett*, 1992, **191**, 527

8 Bakowies, D and Thiel, W, *Chem Phys Lett*, 1992, **193**, 236

9 Taylor, R, *J Chem Soc Perkin Trans* 2, 1992, 1667; Austin, S J *et al J Chem Soc Perkin Trans* 2 1993, 1383

10 Kratschmer, W, Lamb, L D, Fostiropoulous, K, nad Huffman, D R, *Nature*, 1990, **347**, 354

11 Pradeep, T, D'Souza, F, Subbanna, G N, Krishnan, V and Rao C N R, *Proc Indian Acad Sci (Chem Sci)*, 1991, **103**, 685

12 Govindaraj, A and Rao C N R, *Full Sci Technol*, 1993 (in press)

13 Rao, C N R, Bhat, S n and Dwivedi, P C, *Appl Spec Rev* 1971, 5, 1

14 Rathna, A and Chandrasekhar, J, *Chem Phys Lett*, 1993, **206**, 217

ACKNOWLEDGEMENT I thank Prof C N R Rao and Prof J Chandrasekhar for guidance and advice

Received 20 August 1993, revised accepted 27 September 1993

Note added in proof After completing this work, we have become aware of a mass spectrometric study of product distributions of C_{60} - Birch reduction (Banks, M R *et al*, *J Chem Soc. Chem Commun* 1993, 1149)

Evolution of basin boundaries during onset of chaos

G. Ambika*

Department of Physics, Cochin University of Science and Technology, Cochin 682 022, India

The evolution of basin boundaries in a system with multiple attractors is analysed numerically as the system develops period doublings, crises and tangles. The disappearance of the basin of attraction of a chaotic attractor during a boundary crisis as well as the erosion of the bounded basin by the escaping basin due to a heteroclinic tangle are displayed in a series of basin portraits.

IN the study of nonlinear systems, we often come across systems with multiple attractors, i.e. with more than one asymptotically stable states coexisting for one particular set of system parameters. In such cases, each attractor will be having its own separate basin of attraction, the basin being the set of initial points that lead to the attractor as time $t \to \infty$. The boundary of the closure of this region can in general be smooth or fractal. As the attractor undergoes a bifurcation, the basin boundary evolves, either going from a smooth to a fractal or disappearing. Therefore, studies related to the location as well as the nature of these boundaries and their changes as the system parameters evolve have significance because of their implications in the onset of chaos in the system[1–4]. An *a priori* knowledge about how the attractor basins evolve can be of use when we address the question of control mechanisms too, since suitable control is normally applied to bring the system within the basin of a periodic attractor[5]. So, also the extent of basin erosion due to forcing can tell us how far a system has chances of remaining constrained in a noisy environment, and this is a useful criterion in engineering and applied sciences[6, 7].

In this communication, a detailed display of the evolution of basin boundaries of a system with multiple attractors is presented. By concentrating on parameter regimes where interesting phenomena like crises and tangles occur, we study numerically the reorganization of the basin structure as the parameters pass through their critical values. In this context, we note that basin boundary analysis has been carried out extensively in discrete dynamical systems[8–10]. The attractor-basin portraits have been explored in detail recently by Ueda[11] for the Duffing equation, while Thompson *et al.*[12–15] have analysed basin organization prior to escape in a single-well or double-well oscillator.

*On leave from Department of Physics, Maharaja's College, Cochin 682 011, India

The system we have chosen serves as an ideal model for Josephson tunnel junctions. Moreover, it represents the dynamics of a quadratically damped driven pendulum. The governing equation is

$$\ddot{x}+k|\dot{x}|\dot{x}+\sin x = A\sin\omega t. \tag{1}$$

Here x is the dependent variable and a dot above it indicates differentiation with respect to time t. The coefficient k gives the damping constant while A and ω are the amplitude and frequency of the sinusoidal driving force. This system exhibits a rich dynamics as it is made to drift along the parameter space spanned by k, A and ω.

A detailed numerical analysis carried out by us earlier[16, 17] throws light on the possible stable periodic modes and their bifurcations to chaos as the forcing amplitude A is tuned. Here in our discussion we consider the specific case of $k = 0.1$ and concentrate on the basin of attraction of periodic modes of the oscillatory type that occur inside the potential wells of the system. For such modes, $\dot{x}$ averaged over a period is zero or $\langle\dot{x}\rangle = 0$. However, the system in (1) has a series of potential wells centred around the equilibrium points at $(2n\pi, 0)$, with $n = 0, \pm1, \pm2, \ldots$ Since our analysis is mainly on the section of phase space covering the central potential well around (0, 0), the bounded basin considered is that of oscillatory modes around (0, 0). The escape from the well normally leads to rotational modes, which in this particular case may settle down asymptotically to oscillatory modes in other neighbouring wells or to cross-well oscillations as well as chaotic attractors. The pattern of basin changes in each well should be the same but when the central well is under consideration, the basins of attractors in other wells form part of the escaping basin.

When there is no external forcing, i.e. $A = 0$, the system has stable fixed points (or centres) at $(2n\pi, 0)$ and unstable ones or saddles at $((2n+1)\pi, 0)$, with $n = 0, \pm1, \pm2, \ldots$ The stable manifolds W^S of the unstable fixed points at $(\pi, 0)$ and $(-\pi, 0)$ form the boundary between the bounded basin and the escaping basin for the central well, while the upper part of the unstable manifold W^u_A from $(-\pi, 0)$ and the lower part W^u_B from $(\pi, 0)$ approach asymptotically the attractor at (0, 0). For small values of the forcing amplitude A, the fixed point (0, 0) develops into a small stable limit cycle S_n, with the basin boundary remaining practically unaffected. As A is increased, W^u_A from the left saddle L and W^u_B from the right saddle R reorganize themselves and may touch W^s_A of R and W^s_B of L, resulting in a heteroclinic tangency. The value of $A = A_M$ at which this occurs can be computed using Melnikov analysis[18]:

$$A_M = |A - 2k|\cosh(\tfrac{1}{2}\pi\omega) \tag{2}$$

As A is increased beyond A_M, the stable and unstable manifolds accumulate on each other, resulting in a fractal basin boundary. This is referred to as a heteroclinic tangle in the literature[15]. Then we have

$$W^u_A(L)\cap W^s_A(R)\neq\varnothing$$
$$W^u_B(R)\cap W^s_B(L)\neq\varnothing \tag{3}$$

Near the tangle, the system develops a sensitivity to initial conditions, as two nearby points may end up in two widely separated potential wells. The situation, though not exactly chaotic in the strict sense of the word, results in longlived chaotic transients and has been observed in other similar systems[19].

In the present work, fourth-order Runge–Kutta–Gills scheme is used to integrate (1) and since the emphasis is on identifying the asymptotic state and no quantitative measures are computed, the step size chosen is 1/30th of the drive period. The periodic modes S are searched for to fulfil the conditions

$$x\left(\frac{2\pi m}{\omega}\right) = x(0)$$

and

$$\dot{x}\left(\frac{2\pi m}{\omega}\right) = \dot{x}(0). \tag{4}$$

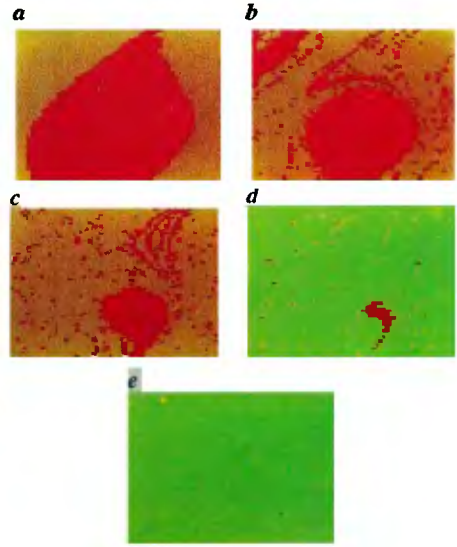

Figure 1. Evolution of basin boundaries during the onset of a reverse boundary crisis. With $k = 0.1$ and $\omega = 0.3$, we study the basins for $A = 0.2, 0.5, 0.8, 1.0, 1.05$. The last figure is taken beyond the crisis point. See text for details regarding the colour

Moreover, for oscillatory modes in the central well, $\langle x \rangle_{\tau_m} = 0$ and $-\pi < x(S_n) < \pi$. The window of phase space considered is $0 < x < 8$ and $-3 < \dot{x} < 3$. The integrations are repeated for a 81×61 grid of initial conditions and the asymptotic states identified after 100 drive cycles. The initial points are then given suitable colours to distinguish the escaping and nonescaping basins.

Our results indicate that for $\omega < 0.5$, the mode excited is a stable nonresonant one, S_n with $m = 1$. Thus, with $\omega = 0.3$ and $A = 0.2$, Figure 1 *a* gives the bounded basin corresponding to S_n in red colour while the yellow regions form the escaping basin belonging to attractors in other wells. The Melnikov threshold in this case is $A_M = 0.2225$. Beyond this, as we increase A values to 0.5 and 0.8, we find a reorganization of the basins affecting mainly the escaping part. However, the bounded basin of S_n suffers a progressive shrinking. Our previous studies indicate that the attractor S_n does not undergo period-doubling bifurcation and the mechanism of onset of chaos that occurs at $A_c = 1.017$ is a reverse boundary crisis[17]. The chaotic attractor that exists for $A > A_c$ collides with the saddle on the basin boundary, resulting in the sudden disappearance of the attractor, leaving only chaotic transients. So the course of events as A is increased is $S_n \rightarrow$ chaotic transients $\rightarrow$ chaos. This is clear from Figure 1 *d* and *e*, just before and after crisis. The green regions in Figure 1 *d* that belong to the chaotic attractor arise due to longlived chaotic transients.

For values of ω lying in the range $0.5 < \omega < 0.9$, a periodic resonant mode S_r is created along with a saddle S_r via a saddle node bifurcation at $A = A_1$ before the Melnikov tangency occurs. The bounded basin is now shared by S_n and S_r and we have a region of resonant hysteresis. This is shown in Figure 2 *a* for $\omega = 0.6$ and $A = 0.3$. The blue colour indicates the newly created basin of S_r which forms a part of the bounded basin. The Melnikov threshold in this case is $A_M = 0.2955$, and as A is increased beyond A_M (Figure 2 *b*–*e*), there is drastic reorganization of the basin of S_r due to the incursion of its basin by escaping basins that belong to S_r or S_n in other wells. Before mass erosion of the basin starts, S_r undergoes a period-doubling bifurcation at $A_B = 0.405$ to an $m = 2$ oscillation and the sequence accumulates at $A = 0.407$. The resulting chaotic attractor disappears[18] via a boundary crisis at $A = 0.411$. Beyond this point, for $A = 0.42$ (Figure 2 *f*) we have only the bounded basin of S_n and the escaping basin shared by the chaotic attractor and attractors in other wells.

If we consider frequencies $\omega > 0.7$, before the period-doubling bifurcation of S_r occurs at A_B, the nonresonant mode S_n disappears in a collision with the saddle S_r at $A = A_2$ and so the bounded basin thereafter is that of S_r alone[18]. Above the Melnikov tangency, long finger-like structures of the escaping basin start penetrating the resonant bounded basin, and as A is increased further, massive erosion of the whole of the bounded basin occurs. These events are shown in Figure 3, where $\omega = 0.8$ and A is increased as $A = 0.2$, 0.35, 0.45, 0.5, 0.55, 0.6, and 0.7. The threshold A_M in this case works out to be 0.3796. Here we also try to display separately the contribution to the escaping basin from the attractors in the different wells, by giving different shades to each one. The bounded basin in the central well is coloured yellow, while the parts of the escaping basin due to attractors in the successive wells on the right are coloured green, violet, red and blue, respectively, with brighter shades of the same colours indicating wells on the left. The white regions correspond to attractors that ultimately escape to rotational modes or chaos. In Figures 3 *a* and *b*, where $A < A_M$, the boundaries are smooth, while in Figure 3 *c* for $A > A_M$, the fractal

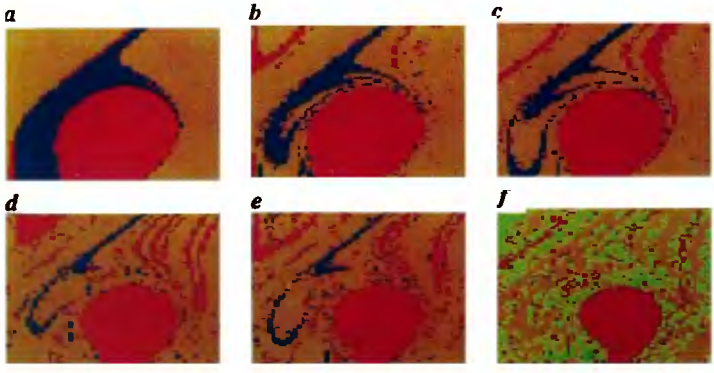

Figure 2. The boundary separating basins of resonant and nonresonant modes inside the central well, for $k = 0.1$ and $\omega = 0.6$ and A-values increase as 0.3, 0.32, 0.34, 0.38, 0.4 and 0.42. Other relevant details are included in the text.

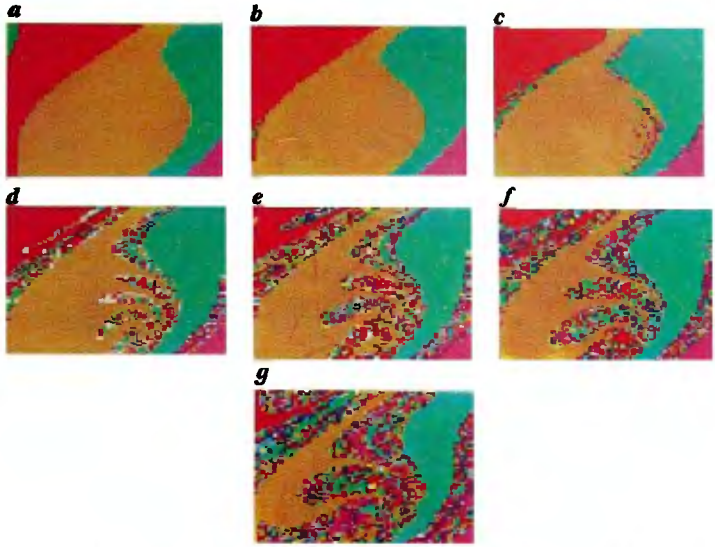

Figure 3. Evolution of the basins of resonant modes inside different wells during the development of a heteroclinic tangle. Here $k = 0.1$ and $\omega = 0.8$. The A-values change sequentially as 0.2, 0.35, 0.45, 0.5, 0.55, 0.6 and 0.7. For a discussion of the colour scheme used, see text.

nature starts forming. Figures 3 *d–g* indicate the erosion of the bounded basin by finger-like structures as the heteroclinic tangle develops. Our previous analysis[17] shows that S_r period doubles at $A_B = 0.95$ and becomes chaotic at $A = 1.02$.

In conclusion, we would like to remark that earlier studies on fractal basin boundaries in pendulum systems relate to the linearly damped case and that too for the frequency-locked rotational modes[20, 21]. There it has been observed that as the rotational modes period-double and approach chaos via an interior crisis, their basins develop fractal boundaries and finally merge together. The fractal structure of the boundaries separating basins of fixed points inside the various wells in a transiently driven pendulum has been studied by Varghese and Thorp[22]. In the present work, we discuss the evolution of the bounded basin inside the central well of a sinusoidally driven pendulum with quadratic damping. Our results for higher frequencies broadly resemble those reported by Soliman and Thompson[23] for periodically driven and linearly damped nonlinear oscillators. We extend the analysis to other frequency regions to include situations where the resonant attractor period doubles before massive erosion of the basin starts. So, also for lower frequencies the reorganization of the basin due to the tangle affects only the escaping basin and the nonresonant bounded basin suffers only a progressive shrinking as the attractor approaches chaos via a reverse boundary crisis.

1. Grebogi, C. and Ott, E., *Phys. Rev. Lett.*, 1983, **50**, 935–938.
2. McDonald, S. W., Grebogi, C., Ott, E. and Yorke, J. A., *Physica*, 1985, **17D**, 125–153.
3. Grebogi, C., Ott, E. and Yorke, J. A., *Physica*, 1987, **24D**, 243–262.
4. Rajasekar, S. and Lakshmanan, M., *Phys. Lett.*, 1990, **A147**, 264–268.
5. Rajasekar, S. and Lakshmanan, M., *Int. J. Bifur. Chaos*, 1992, **2**, 201–204.
6. Thompson, J. M. T. and Ueda, Y., *Dynamics and Stability of Systems*, 1989, **4**, 285–294.
7. Soliman, M. S. and Thompson, J. M. T., *Int J. Bifur. Chaos*, 1992, **2**, 81–91.
8. Grebogi, C., Ott, E. and Yorke, J. A., *Physica*, 1983, **7D**, 181–200.
9. Valkering, T. P., *Physica*, 1986, **18D**, 483–485.
10. Yamaguchi, Y. and Tanikawa, K., *Phys. Lett.*, 1989, **A142**, 95–98.
11. Ueda, Y., *Chaos Solitons & Fractals*, 1991, **1**, 199–231.
12. Moon, F. C. and Li, G. X., *Phys. Rev. Lett.*, 1985, **55**, 1439–1442.
13. Thompson, J. M. T., Bishop, S. R. and Leung, L. M., *Phys. Lett.*, 1987, **A121**, 116–120.
14. Lansbury, A. N. and Thompson, J. M. T., *Phys. Lett.*, 1990, **A150**, 355–361.
15. Soliman, M. S. and Thompson, J. M. T., *Int. J. Bifur. Chaos*, 1991, **1**, 107–118.
16. Ambika, G., Babu Joseph, K. and Nandakumaran, V. M., *Mod. Phys. Lett.*, 1991, **B5**, 519–530; Errata: *Mod. Phys. Lett.*, 1991, **B5**, 1037–1039.
17. Ambika, G., *J. Phys. Condens. Matter*, 1992, **4**, 4829–4838.
18. Xiao, W. and Yao, X., *Act. Phys. Sin.*, 1989, **38**, 137–147.
19. Li, G. X. and Moon, F. C., *J. Sound Vib.*, 1990, **136**, 17–34.
20. Gwinn, E. G. and Westervelt, R. M., *Phys. Rev.*, 1986, **A33**, 4143–4155.

21 Grebogi C, Ott E and Yorke J A, *Phys Rev Lett*, 1986, **56**, 1011–1014
22 Varghese M and Thorp, J S, *Phys Rev Lett*, 1988, **60**, 565–568
23 Soliman M S and Thompson, J M T, *Phys Rev*, 1992, **A45**, 3425–3431

ACKNOWLEDGEMENTS. This work was supported by the Council of Scientific and Industrial Research, New Delhi, through a research associateship. The technical assistance of R. Sivakumar, NPOL, Cochin during computations is acknowledged.

Received 12 April 1993, revised accepted 8 September 1993

Rotifers – pollution or productivity indicators?

A. K. Laal and M. Karthikeyan

Reservoir Division, CICFRI (ICAR), 22, 1st Main, 4th Block, Rajajinagar, Bangalore 560 010, India

In order to test whether rotifers are most efficient as pollution or productivity indicators, impact of abiotic parameters and primary productivity on abundance of rotifers was studied. Population of rotifers was found to be more in polluted zone with numerical superiority of *Brachionus rubens* and *Brachionus angularis*. Different inter-correlations were estimated and from multiple regression analysis it was observed that rotifers were influenced most by chloride, which is an index of pollution.

ROTIFERS as component of zooplankton are widely distributed. Since they are very sensitive to ambient ecosystem, they are used as bio-indicators in monitoring pollution[1–7] and productivity[8–12]. To ascertain whether rotifers are bio-indicators more of pollution or productivity, we have investigated the inter-relations of abiotic parameters including chloride (pollution indicator) and primary productivity on abundance of rotifers.

The study was conducted during September 1979 and February 1982 at clean and polluted sites of river Ganga at Bhagalpur (25°14′ N; 86°57′ E)[6,7]. Hydrobiological samples were collected at monthly intervals and were subsequently analysed. Data on temperature, pH, dissolved oxygen, total alkalinity, dissolved organic mater, chloride, primary productivity and rotifers from both zones were pooled together and analysed for estimating different inter-correlations. The data were also subject to multiple regression analysis.

Out of 22 taxa of rotifers available in this stretch, eight rotifers, viz. *Keratella tropica, Brachionus calyciflorus, B forficula, B. falcatus, B. caudatus, Anuraeopsis fissa, Polyarthra ehrenburg* and *Filinia terminalis*, were found both in clean and polluted zones. They seem to be tolerant to wide fluctuations of abiotic parameters and hence they are being used as indicators of both polluted and productive waters. The remaining 14, viz. *Brachionus rubens, B angularis, B bakeri, B urceolaris, Lepadella ovalis, Platyas patulus, Porales* sp., *Rotaria rotatoria, Asplanehna brightwell, Horaella brehmi, Filinia longispina, F. opoliensis, Lecane ohiensis and Mytilina ventralis* were confined to polluted zone. Amongst them *B rubens* and *B angularis* occur in swarms. A shift in species composition of rotifers from clean to polluted zones was apparent.

Inter-relations of abiotic parameters and primary productivity on abundance of rotifers are given in Table 1. The correlation analysis showed that correlation coefficients of rotifers with water temperature ($r = 0.398$), chloride ($r = 0.304$) and primary productivity ($r = 0.296$) were statistically significant at 5% level. From multiple regression analysis (with logarithmic transformation), it was observed that the effect of chloride on rotifers was statistically significant at 5% level. Multiple regression fitted to the observed data was:

$$\log Y = -7.146 + 1.438 \log X_1 + 1.396 \log X_2 + 0.236 \log X_3$$
$$(1.037) \qquad (0.278) \qquad (0.185)$$
$$(n = 51,\ R^2 = 0.47)$$

where X_1, X_2, X_3 and Y represent water temperature, chloride, primary productivity and rotifers respectively. Figures within parenthesis indicate the standard error of the respective regression coefficients.

From the estimates of standard partial regression coefficients[19] it was observed that abundance of rotifers

Table 1 Correlation matrix

	Temp	pH	DO	T Alk	DOM	Cl	GP	Rotif
Temp	1.000*	0.083	–0.194	0.061	–0.320*	0.090	0.345*	0.398*
pH	0.083	1.000*	0.075	0.024	–0.147	0.208	0.232	0.197
DO	–0.194	0.075	1.000*	–0.460*	–0.208	–0.614*	–0.356*	–0.255
T Alk	0.061	0.024	–0.460*	1.000*	0.368*	0.642*	0.296*	0.037
DOM	–0.320*	–0.147	–0.208	0.368*	1.000*	0.331*	0.178	–0.066
Cl 0.090	0.208	–0.614*	0.642*	0.331*	1.000*	0.542*	0.304*	
GP	0.345*	0.232	–0.356*	0.296*	0.178	0.542*	1.000*	0.296*
Rotif	0.398*	0.197	–0.255	0.037	–0.66	0.304*	0.296*	1.000*

* Indicate significance at 5% level.